AD-A048 363 AIR FORCE INST OF TECH WRIGHT-PATTERSON AFB OHIO SCH--ETC F/G 20/4
APPLICATION OF THE KARMAN-POHLHAUSEN METHOD TO THE EXTENDED BOU--ETC(U)
DEC 77 R D BEHR

UNCLASSIFIED AFIT/GAE/AA/77D-1 NL

| OF |
ADA048363

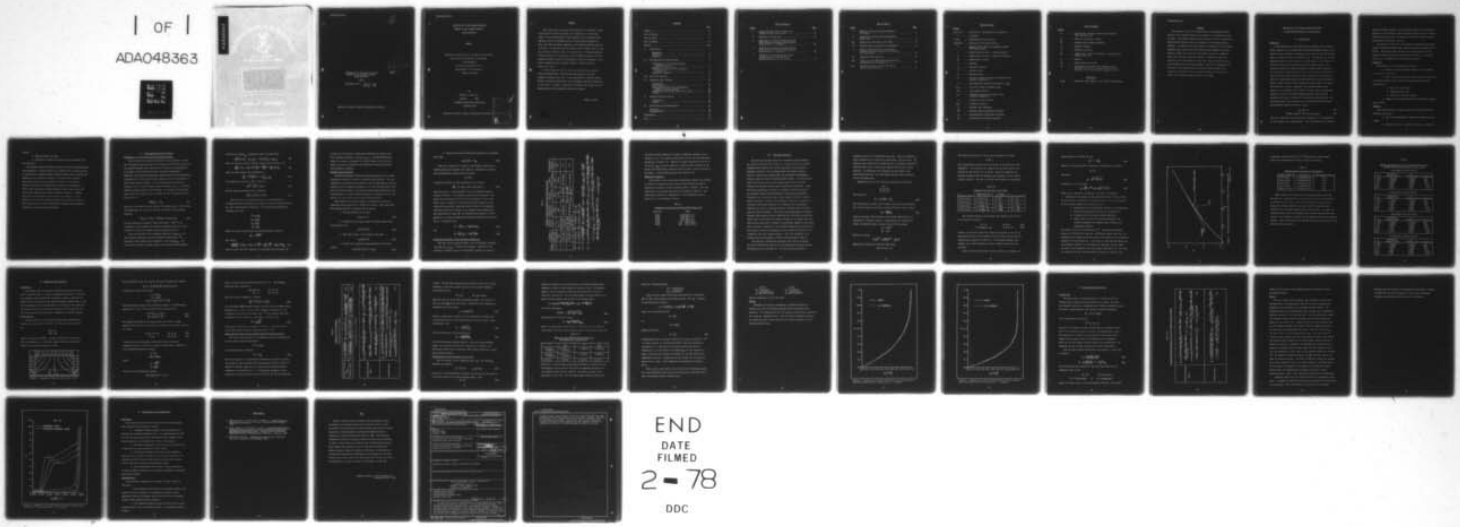

END
DATE FILMED
2-78
DDC

AFIT/GAE/AA/77D-1

APPLICATION OF THE KARMAN-POHLHAUSEN METHOD TO THE EXTENDED BOUNDARY LAYER EQUATIONS

Thesis

AFIT/GAE/AA/77D-1 Robert D. Behr
Captain USAF

AFIT/GAE/AA/77D-1

APPLICATION OF THE KARMAN-POHLHAUSEN METHOD TO THE EXTENDED BOUNDARY LAYER EQUATIONS

THESIS

Presented to the Faculty of the School of Engineering
of the Air Force Institute of Technology
Air University
in Partial Fulfillment of the
Requirements for the Degree of
Master of Science

by

Robert D. Behr, B.S.
Captain USAF
Graduate Aeronautical Engineering

December 1977

Approved for public release; distribution unlimited.

Preface

This study was an analytical investigation of the laminar, steady, two-dimensional extended boundary layer equations at low Reynolds number. The extended boundary layer equations are the Navier-Stokes equations with the assumption that the normal pressure gradient is zero, such that the normal component of the momentum equation need not be solved. This differs from the boundary layer equation model in that the streamwise diffusion term is not neglected. An "extended momentum integral equation" was developed from the continuity equation and the streamwise momentum equation and applied to three flow problems - flat plate, stagnation point, circular cylinder - using the Karman-Pohlhausen method.

I would especially like to thank my thesis advisory committee, Professor Richard Merz and Professor Harold Wright, for their guidance throughout this task. I also would like to thank my faculty advisor, Professor Stephen Koob, for his guidance and much needed help in this study. Finally, I would like to thank my wife, Karen, for her understanding and encouragement during this project.

Robert D. Behr

Contents

List of Figures

List of Tables

List of Symbols

Symbol

a,b,c,d,e	. . . functions of x determined in the analysis
C	. . . a constant
erfc	. . . complementary error function
$f(y),F(y)$	. . . functions in the exact solution
h	. . . height of layer which is everywhere outside the boundary layer
J	. . . dimensionless quantity - pressure gradient
K	. . . dimensionless quantity - streamwise diffusion
ℓ	. . . characteristic length
p	. . . pressure
p_0	. . . stagnation pressure
R	. . . cylinder radius
Re	. . . Reynolds number
u,v	. . . velocity components tangent and normal to the surface, respectively
U	. . . non-dimensional velocity distribution, U_e/U_∞
U_e,V_e	. . . velocity at edge of boundary layer
U_∞	. . . free stream velocity
x,y	. . . coordinates tangent and normal to the surface, respectively
α	. . . constant in exact solution
β,γ	. . . numerical constants
δ	. . . boundary layer thickness
δ^*	. . . boundary layer displacement thickness
δ_1	. . . non-dimensional displacement thickness
δ_2	. . . non-dimensional momentum thickness

List of Symbols

Symbol

η	. . . cross-stream coordinate referenced to boundary layer thickness, y/δ
η_δ	. . . value of η where $U_e = .99\ U_\infty$
θ	. . . boundary layer momentum thickness
μ	. . . dynamic viscosity
ν	. . . kinematic viscosity
ξ	. . . stream-wise coordinate referenced to characteristic length, x/ℓ or x/R
ρ	. . . density
τ_w	. . . shear stress at the wall
ϕ	. . . angle defining position from stagnation point in degrees on circular cylinder and dimensionless function in exact solution for stagnation point

Subscripts

x,y,ξ	. . . derivative with respect to x,y, and ξ, respectively

Abstract

An analytical study of the application of the Karman-Pohlhausen method to the extended boundary layer equations at low Reynolds number was made. The extended boundary layer equations were the incompressible Navier-Stokes equations with the assumption of zero normal pressure gradient. A comparison was made between the solutions for the extended boundary layer equations and the boundary layer equations at several Reynolds numbers for flow over a flat plate, flow near a stagnation point, and flow over a circular cylinder. Favorable results were achieved for the flat plate case while less than satisfactory results were achieved for the circular cylinder. The point of separation was not found. Any further study in this area should consider using cylindrical coordinates for the cylinder solution and examining the effect of the pressure gradient normal to the body.

APPLICATION OF THE KARMAN-POHLHAUSEN METHOD TO THE EXTENDED BOUNDARY LAYER EQUATIONS

I. Introduction

Background

In the derivation of the boundary layer equations from the Navier-Stokes equations it is assumed that the pressure gradient normal to the surface is zero such that the pressure at the outer edge of the boundary layer is impressed across the boundary layer. Furthermore, the velocity component parallel to the surface, u, becomes equal to the velocity of the outer flow, U_e, at the outer edge of the boundary layer. The resulting equations are known as Prandtl's boundary layer equations. For low Reynolds number flows and in many other situations (particularly large adverse pressure gradients), these equations do not adequately model the fluid physics and the full Navier-Stokes equations should be solved. However, due to their coupled non-linear nature, they remain very difficult to solve. Therefore, the extended boundary layer equations are introduced in an attempt to retain some of the physical modeling accuracy of the Navier-Stokes equations along with the simplicity and ease of solution of the boundary layer equations. The extended boundary layer equations are the two-dimensional continuity and streamwise momentum equations, namely,

$$u_x + v_y = 0 \tag{1}$$

$$\rho(uu_x + vu_y) = -p_x + \mu(u_{xx} + u_{yy}) \tag{2}$$

where the streamwise viscous diffusion term, μu_{xx}, is not neglected as in the boundary layer approximation. This work addresses an "extended

momentum integral equation" for the extended boundary layer equations analogous to the classical momentum integral equation for the boundary layer equations and solves the equation for several external pressure distributions and Reynolds numbers.

The problem of flow over a flat plate has previously been solved using the extended boundary layer equations by Koob and Abbott (Ref 2: 64-77). This previous work was used as a starting point once the momentum integral equation was developed and served as a procedural check prior to examining the more difficult problems.

Objectives

The objectives of this work were as follows:

1. Develop a momentum integral equation for the extended boundary layer equations.

2. Solve the extended momentum integral equation numerically for several Reynolds numbers and the following external pressure distributions:

   a. Flow over a flat plate.

   b. Stagnation point flow.

   c. Flow over a circular cylinder.

3. Compare the extended boundary layer and Prandtl boundary layer results.

Approach

The extended momentum integral equation was developed with the following assumptions:

1. Flow was two-dimensional, laminar, incompressible, and steady.

2. Pressure was only a function of distance, x, along the

surface.

3. Reynolds number was small.

4. Interaction between the external flow and boundary layer was negligible.

The extended momentum integral equation was then non-dimensionalized and polynomials of various degrees were assumed for the velocity profile to transform the extended momentum integral equation from a differential equation in four dependent variables to a second order, ordinary differential equation in one dependent variable. The dependent variable used was the non-dimensional displacement thickness, δ_1. A fourth order Runge-Kutta computer program was then used to solve the differential equation with specified initial conditions. Boundary layer and extended boundary layer results were compared. It was desired to show that the extended boundary layer equations would be a more accurate model of fluid flows than the boundary layer equations, especially in adverse pressure gradients.

II. The Approximate Solution Method

Development of the Extended Momentum Integral Equation

Since the full Navier-Stokes equations are very difficult to solve and the boundary layer equations do not apply near and beyond separation, the extended boundary layer equations, Eq 1 and Eq 2, were proposed as a new model to meet accuracy and ease of solution requirements. Basically, the extended boundary layer equations were the two-dimensional, incompressible, steady, Navier-Stokes equations with the assumption of a zero normal pressure gradient. From the two-dimensional continuity equation, Eq 1, and the streamwise momentum equation, Eq 2, an "extended momentum integral equation" was developed. At the edge of the boundary layer, where the boundary layer has merged with the external flow, Eq 2 had the form:

$$\rho U_e U_{e_x} = - p_x \tag{3}$$

where U_e is the velocity at the edge of the boundary layer. Substituting the relationship for p_x in Eq 3 into Eq 2 resulted in the following equation:

$$\rho u u_x + \rho v u_y = \rho U_e U_{e_x} + \mu (u_{xx} + u_{yy}) \tag{4}$$

The same procedure described in Schlichting (Ref 3: 145) for the development of the boundary layer momentum integral equation was then followed to develop the extended momentum integral equation.

With the inclusion of the streamwise diffusion term, μu_{xx}, the final equation differed from that presented in Schlichting. Two additional terms appeared from integration of the term, μu_{xx}. The form of this term was as follows (after Eq 4 had been divided through

by ρ and the term $\sqrt{U_{e_{xx}}}$ introduced to aid the integration):

$$-\sqrt{\int_0^h ([U_e - u]_{xx} - U_{e_{xx}})\, dy} = -\sqrt{(U_e \delta^*)_{xx}} + \sqrt{U_{e_{xx}}}\, h \tag{5}$$

Thus, the extended momentum integral equation was developed to be

$$\frac{\tau_w}{\rho U_e^2} = \theta_x + (2\theta + \delta^*)\frac{U_{e_x}}{U_e} + \frac{\sqrt{U_{e_{xx}}}\, h}{U_e^2} - \frac{\sqrt{}}{U_e^2}(U_e \delta^*)_{xx} \tag{6}$$

where the shear stress, τ_w, is defined by

$$\frac{\tau_w}{\rho} = \frac{\mu u_y|_{y=0}}{\rho} = -\sqrt{\int_0^h u_{yy}\, dy} \tag{7}$$

the displacement thickness, δ^*, is defined by

$$U_e \delta^* = \int_0^h (U_e - u)\, dy \tag{8}$$

and the momentum thickness, θ, is defined by

$$U_e^2 \theta = \int_0^h u(U_e - u)\, dy \tag{9}$$

Since Eq 6 was in a dimensional form, it was advantageous to non-dimensionalize the equation with respect to the free stream velocity, U_∞, and a characteristic length, ℓ. The following non-dimensional variables were used:

$$U = U_e / U_\infty$$

$$\delta_1 = \delta^*/\ell$$

$$\delta_2 = \theta/\ell$$

$$\xi = x/\ell$$

Making the proper substitutions and defining Reynolds number as

$$Re = \frac{\rho U_\infty \ell}{\mu}$$

Eq 6 became

$$\frac{u_y|_{y=0}\,\ell}{Re\, U U_e} = (\delta_2)_\xi + (2\delta_2 + \delta_1)\frac{U_\xi}{U} + \frac{\delta}{Re\,\ell}\frac{U_{\xi\xi}}{U} - \frac{1}{Re\, U^2}(U\delta_1)_{\xi\xi} \tag{10}$$

where h in Eq 6 has been replaced by the boundary layer thickness, δ.

As seen, Eq 10 was still a second order differential equation with four dependent variables - δ, δ_1, δ_2, $u_y \mid_{y=0}$. The Karman-Pohlhausen method of assuming a polynomial of various degrees for the velocity profile was used to establish three additional relationships among these dependent variables.

Assumed Velocity Profiles

The Karman-Pohlhausen method has been demonstrated to be a useful approximate method for solving the boundary layer equations. The same techniques and conditions were applied to the extended momentum integral equation, Eq 10, assuming polynomials of the first through fourth degree for the velocity profile. The first and second degree polynomials were used primarily to establish those procedures in integration which would provide the best results for the other velocity profiles.

When choosing the velocity profile, consideration was given to requiring certain properties or conditions to exist. These were taken from Schlichting (Ref 3: 193) and were as follows:

1. No-slip condition at the wall.

$$u(x,o) = 0 \tag{11}$$

2. Continuity at the point where the boundary layer meets the potential flow.

$$u(x,\delta) = U_e \tag{12}$$

3. Zero shear stress at the boundary layer edge.

$$u_y(x,\delta) = 0 \tag{13}$$

4. Satisfy the streamwise momentum equation at the body surface.

$$\nu u_{yy}(x,o) = \frac{1}{\rho} p_x = -U_e U_{e_x} \tag{14}$$

5. Satisfy the inviscid (potential) equation at the boundary layer edge.

$$u_{yy}(x,\delta) = -U_{e_{xx}} \tag{15}$$

With Eq 11 through Eq 15 serving as the boundary conditions, a velocity profile was assumed in the form of a polynomial in terms of the non-dimensional distance from the surface

$$\eta = y/\delta$$

A general expression for this polynomial was as follows:

$$u/U_e = a + b\eta + c\eta^2 + d\eta^3 + e\eta^4 + \ldots \tag{16}$$

where a,b,c,d,e,... were functions of x to be evaluated from the boundary conditions. The boundary conditions used depended on the degree of the polynomial selected and the judgement of the author. Table I gives a summary of the velocity profiles examined in this study with the boundary conditions used and three of the dependent variables defined as functions of the boundary layer thickness, δ, and characteristic length, ℓ. The dimensionless quantities J and K appeared as a result of applying the boundary conditions of Eq 14 and Eq 15. In equation form,

$$J = \frac{\delta^2}{\nu} U_{e_x} = (\delta/\ell)^2 \, Re \, U_\xi \tag{17}$$

and

$$K = \frac{\delta^2}{U_e} U_{e_{xx}} = (\delta/\ell)^2 \frac{U_{\xi\xi}}{U} \tag{18}$$

Differential Equation in One Dependent Variable, δ_1

With the velocity profile assumed, the four dependent variables - δ, δ_1, δ_2, and $u_y \big|_{y=0}$ - in Eq 10 were related. Therefore it was possible to represent three of the dependent variables in terms of

Table I

Summary of Velocity Profile Properties and Results

Degree	Boundary Conditions	Velocity Profile	Displacement Thickness, δ_1	Momentum Thickness, δ_2	Shear Stress, $u_y\big\|_{y=0}$	Differential Equation
1	(11),(12)	η	$\delta/2\ell$	$\delta/6\ell$	U_e/δ	(19)
2	(11),(12),(13)	$2\eta-\eta^2$	$\delta/3\ell$	$2\delta/15\ell$	$2U_e/\delta$	(20)
3	(11),(12),(13),(14)	$(\frac{3}{2}+\frac{J}{4})\eta-\frac{J}{2}\eta^2+(-\frac{1}{2}+\frac{J}{4})\eta^3$	$(\frac{3}{8}-\frac{J}{48})\delta/\ell$	$(\frac{39}{280}-\frac{J}{560}-\frac{J^2}{1680})\delta/\ell$	$(\frac{3}{2}+\frac{J}{4})U_e/\delta$	(21)
4	(11),(12),(13),(14),(15)	$(2+\frac{J}{6}-\frac{K}{6})\eta-\frac{J}{2}\eta^2+(-2+\frac{J}{2}+\frac{K}{2})\eta^3+(1-\frac{J}{6}-\frac{K}{3})\eta^4$	$(\frac{3}{10}-\frac{J}{120}+\frac{K}{40})\delta/\ell$	$(\frac{37}{315}-\frac{J}{945}-\frac{J^2}{9072}+\frac{11\,71K}{3780}+\frac{5JK}{9072}-\frac{19K^2}{22680})\delta/\ell$	$(2+\frac{J}{6}-\frac{K}{6})U_e/\delta$	(22)

(19) $$\delta_1'' = \delta_1'\left(\tfrac{1}{3}ReU - \frac{2U'}{U}\right) + \delta_1\left(\tfrac{5}{3}ReU' + \frac{U''}{U}\right) - \frac{1}{2\delta_1}$$

(20) $$\delta_1'' = \delta_1'\left(\tfrac{2}{5}ReU - \frac{2U'}{U}\right) + \delta_1\left(\tfrac{9}{5}ReU' + \frac{2U''}{U}\right) - \frac{2}{3\delta_1}$$

(21) $$\delta_1'' = \delta_1'\left(\frac{[39-J/2-J^2/6]ReU}{35[3-J/6]} - \frac{2U'}{U}\right) + \delta_1\left(\left\{\frac{2[39-J/2-J^2/6]}{35[3-J/6]}+1\right\}ReU' + \frac{J'ReU[5-J+J^2/36]}{35[9-J+J^2/36]} + \left[\frac{8}{(3-J/6)}-1\right]\frac{U''}{U}\right) - \frac{(9+J-J^2/12)}{16\delta_1}$$

(22) $$\delta_1'' = \delta_1'\left(\frac{10ReU\left[\frac{37}{315}-\frac{J}{945}-\frac{J^2}{9072}+\frac{11\,71K}{3780}+\frac{5JK}{9072}-\frac{19K^2}{22680}\right]}{[3-J/12+K/4]} - \frac{2U'}{U}\right) + \delta_1\left(ReU'\left[\frac{20\left(\frac{37}{315}-\frac{J}{945}-\frac{J^2}{9072}+\frac{11\,71K}{3780}+\frac{5JK}{9072}-\frac{19K^2}{22680}\right)}{(3-J/12+K/4)}\right.\right.$$
$$\left. + 1\right] + \left[\frac{10}{(3-J/12+K/4)}-1\right]\frac{U''}{U} + 10ReU\left[\frac{(3-J/12+K/4)(-J'/945-2JJ'/9072+11\,71K'/3780+5J'K/9072+5JK'/9072-19KK'/11340)}{(3-J/12+K/4)^2}\right.$$
$$\left.\left. - \frac{\left(\frac{37}{315}-\frac{J}{945}-\frac{J^2}{9072}+\frac{11\,71K}{3780}+\frac{5JK}{9072}-\frac{19K^2}{22680}\right)(-J'/12+K'/4)}{(3-J/12+K/4)^2}\right]\right) - \frac{(2+J/6-K/6)(3-J/12+K/4)}{10\delta_1}$$

the fourth thereby reducing the number of dependent variables in the equation to one. The variable selected for use was the non-dimensional displacement thickness, δ_1. Making the proper substitutions into Eq 10 for δ_2 and $u_y|_{y=0}$ for each respective velocity profile resulted in the second order differential equations listed in Table I as Eq 19 to Eq 22. The symbol ' infers differentiation with respect to η.

Numerical Integration

The solution to the second order differential equation was obtained by numerical integration using a fourth order Runge-Kutta computer program as discussed in Ketter and Prawel (Ref 1: 268-277). The step sizes used in the program were adjusted according to Table II. Any additional constraints or requirements on the integration will be discussed in the appropriate sections.

Table II

Integration Step Size and Corresponding Range of η

Step Size	Range
η/10	$0.000 \leq \eta < 0.01$
0.005	$0.010 \leq \eta < 1.0$
0.010	$1.000 \leq \eta < 5.0$
0.050	$5.0 \leq \eta < 10.0$
0.100	$10.0 \leq \eta < 100.0$
0.500	$100.0 \leq \eta < 1000.0$

III. Flat Plate Solution

The flat plate problem which has no external pressure gradient was solved by Koob and Abbott (Ref 2). In their study, the extended boundary layer equations were solved numerically by requiring the numerical solution to form a bridge between the Stokes solution, which is valid near the leading edge, and the Prandtl approximation solution, which is valid for large Reynolds numbers. An initial δ_1 was chosen sufficiently close to the leading edge so that the Stokes equation and extended boundary layer equation were equivalent. Using the Stokes approximation solution to determine starting conditions, the extended boundary layer differential equation was numerically integrated in an attempt to reach a point where the Blasius solution would be realized. However, the integration could not be carried far enough for the Blasius character to be apparent and an asymptotic expansion was used for ξ greater than 45 to compute δ_1 and eventually reach the Blasius solution. The results from integrating the extended boundary layer equations were in agreement with the Stokes solution for ξ less than 0.25 and with the Prandtl solution for ξ greater than 100. These results were used to evaluate the procedures applied in this study and to provide a comparison of the extended boundary layer solutions for this simple case before undertaking the more difficult problems of the stagnation point and circular cylinder. Thus, the procedures to be followed here were analogous to those in Koob and Abbott (Ref 2).

The applicable differential equations came from Eq 19 through Eq 22 with substitution made for the non-dimensional external pressure distribution and its derivatives. For the flat plate problem, U

equaled one and all its derivatives were zero. Thus, the variables J and K, defined by Eq 17 and Eq 18, respectively, were also zero. The equations were significantly simplified and the techniques employed by Koob and Abbott (Ref 2: 66-70) were applied for all four velocity profiles. To demonstrate the techniques, as they apply to the differential equations, the third degree velocity profile equation will be developed here.

Beginning with Eq 21 the following substitutions were made:

$$U = 1$$
$$U' = U'' = 0$$
$$J = J' = 0$$

The result was

$$\delta_1'' = \delta_1' \left(\frac{13\,Re_2}{35}\right) - \frac{9}{16\,\delta_1} \tag{23}$$

The corresponding boundary layer equation was derived by neglecting the last two terms in Eq 10 or by setting δ_1'' equal to zero in Eq 23

$$\delta_1' = \frac{315}{208\,Re\,\delta_1} \tag{24}$$

Since the boundary layer equations were usually transformed to be independent of Reynolds number, a transformation was performed to remove the Reynolds number from Eq 23 and Eq 24 by assuming

$$\bar{\delta}_1 = \delta_1 Re^{\beta}$$
$$\bar{\xi} = \xi Re^{\gamma}$$

Equation 23 became

$$\bar{\delta}_1'' Re^{2\gamma-\beta} = \bar{\delta}_1' \left(\frac{13}{35}\right) Re^{\gamma-\beta+1} - \frac{9}{16\bar{\delta}_1} Re^{\beta}$$

Equating the exponents of Reynolds number gave

$$2\gamma - \beta = \gamma - \beta + 1 = \beta$$

from which the values of γ and β were determined to be unity

$$\gamma = \beta = 1$$

This transformation resulted in Eq 23 and Eq 24 being Reynolds number independent. The procedure was repeated for the other profiles and yielded the same results for γ and β. Table III summarizes the extended boundary layer and boundary layer equations for the various velocity profiles. The bars on δ_1 have been dropped for convenience.

Table III

Equations for Flow Over a Flat Plate

Velocity Profile	Extended Boundary Layer Equation	Boundary Layer Equation	Stokes Equation
First degree	$\delta_1'' = \delta_1'(\frac{1}{2}) - \frac{1}{2\delta_1}$	$\delta_1' = \frac{3}{2\delta_1}$	$\delta_1'' = -\frac{1}{2\delta_1}$
Second degree	$\delta_1'' = \delta_1'(\frac{2}{5}) - \frac{2}{3\delta_1}$	$\delta_1' = \frac{5}{3\delta_1}$	$\delta_1'' = -\frac{2}{3\delta_1}$
Third degree	$\delta_1'' = \delta_1'(\frac{13}{35}) - \frac{9}{16\delta_1}$	$\delta_1' = \frac{315}{208\delta_1}$	$\delta_1'' = -\frac{9}{16\delta_1}$
Fourth degree	$\delta_1'' = \delta_1'(\frac{74}{189}) - \frac{3}{5\delta_1}$	$\delta_1' = \frac{567}{370\delta_1}$	$\delta_1'' = -\frac{3}{5\delta_1}$

The extended boundary layer equation was singular for the first of two boundary conditions

$$\delta_1 = 0 \qquad \text{at } \xi = 0 \qquad (25)$$

$$\delta_1 \longrightarrow \text{Blasius Limit} \qquad \text{at } \xi \longrightarrow \infty \qquad (26)$$

However, two solutions which were valid near ξ equal to zero and ξ approaching infinity were determined from the Stokes equation and the boundary layer equation in Table III. The extended boundary layer equation was solved numerically to form a bridge between these two solutions.

Again using the third degree velocity profile as an example, the

Stokes equation from Table III was

$$\delta_1'' = -\frac{9}{16\delta_1} \tag{27}$$

Equation 27 was analytically integrated by introducing the variable

$$p = \delta_1'$$

such that,

$$p = \sqrt{C - \frac{9}{8}\ln\delta_1} \tag{28}$$

Integration of Eq 28 yielded

$$\xi = \sqrt{\frac{8\pi}{9}}\, e^{8/9\, C}\, \mathrm{erfc}\left(\sqrt{8/9\, C - \ln\delta_1}\right) \tag{29}$$

where C was a constant of integration which must be evaluated.

Following the procedures of Koob and Abbott (Ref 2: 71), Eq 28 and Eq 29 were used to determine the initial conditions for the integration of the extended boundary layer equation, Eq 23.

1. Pick values for the integration constant, C, and initial δ_1.
2. Solve Eq 28 and Eq 29 for δ_1' and ξ, respectively.
3. Integrate Eq 23 with these initial conditions.
4. Adjust value of C until the extended boundary layer solution approaches the boundary layer solution at ξ approaching infinity.

The initial value of δ_1 selected was 10^{-12}. During the integration process if δ_1' became less than zero or δ_1'' became greater than zero, the integration was stopped since this would be in violation of the asymptotic behavior of δ_1 (See Figure 1). A new value of C was then determined and the procedure repeated. It was during this procedure that the range and size of the integration step were refined (See Table II). The value of C differed for each velocity profile; however, the limits in the

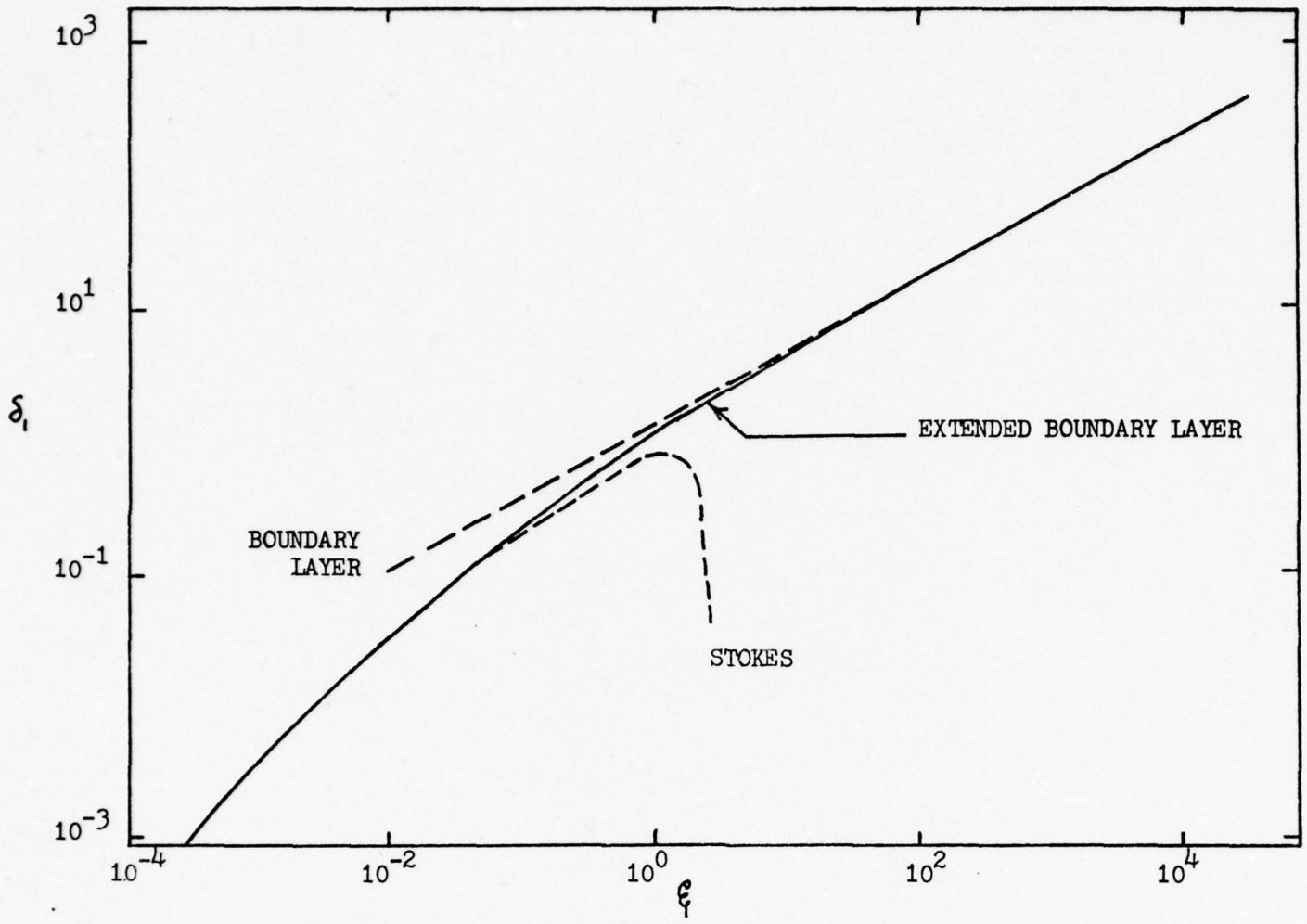

Figure 1. Extended Boundary Layer Solution for Steady Flow Over a Flat Plate (From Ref 2: 74)

integration procedure before δ_1' or δ_1'' exceeded the aforementioned limits were approximately the same as Table IV indicates.

Table IV

Constant Values and Limits of Integration

Velocity Profile	Constant, C	ξ Integration Limit
First degree	-0.16689083968326	76.5
Second degree	-0.27382846491445	65.8
Third degree	-0.24323951331955	67.7
Fourth degree	-0.28399250520450	55.0
Blasius (Ref 2)	-0.24488597951216	70.0

Table V depicts the results of the extended boundary layer and boundary layer approximations for each case and the per cent difference as compared to each other. This per cent difference was computed by taking the difference between the values of the two solutions and dividing by the extended boundary layer solution value. As shown, the extended boundary layer and boundary layer solutions agreed within five per cent of one another at ξ =50, but for smaller ξ the error increased rapidly. These same results were obtained by Koob and Abbott (Ref 2: 75) using the Blasius profile.

Table V

Results and Comparison of the Extended Boundary Layer and Boundary Layer Solutions for a Flat Plate

First Degree Velocity Profile

ξ	δ_1 Extended Boundary Layer	δ_1 Boundary Layer	% Difference
0.001	0.002588	0.05477	2016.
0.01	0.02138	0.1732	710.
0.1	0.1606	0.5477	241.
1.0	1.003	1.732	72.7
10.0	4.667	5.477	17.35
50.0	11.620	12.247	5.39

Second Degree Velocity Profile

ξ	δ_1 Extended Boundary Layer	δ_1 Boundary Layer	% Difference
0.001	0.002950	0.05774	1857.
0.01	0.02424	0.1826	653.
0.1	0.1801	0.5774	220.
1.0	1.102	1.826	65.7
10.0	5.007	5.774	15.30
50.0	12.330	12.910	4.70

Third Degree Velocity Profile

ξ	δ_1 Extended Boundary Layer	δ_1 Boundary Layer	% Difference
0.001	0.002724	0.05503	1920.
0.01	0.02243	0.1740	675.
0.1	0.1675	0.5503	229.
1.0	1.033	1.740	68.4
10.0	4.740	5.503	16.10
50.0	11.723	12.306	4.97

Fourth Degree Velocity Profile

ξ	δ_1 Extended Boundary Layer	δ_1 Boundary Layer	% Difference
0.001	0.002803	0.05536	1875.
0.01	0.02304	0.1751	660.
0.1	0.1715	0.5536	222.
1.0	1.052	1.751	66.4
10.0	4.792	5.536	15.52
50.0	11.816	12.379	4.76

IV. Stagnation Point Solution

Introduction

The boundary layer flow around a shaped body generally proceeds from a stagnation point to a point of separation and beyond. Therefore, the stagnation point problem was considered in order to establish the proper initial conditions for the circular cylinder problem which is seen as the principal test of the new method. The discussion was limited to the assumed third and fourth degree polynomial velocity profiles since the lower degree profile shapes were independent of pressure gradient.

Exact Solution

An exact solution to the complete Navier-Stokes equations was found by K. Hiemenz (Ref 3: 87-90). The potential flow was defined by

$$U_e = a x$$
$$V_e = -a y$$

where "a" denotes a constant. As shown in Figure 2, the potential flow, perpendicular to a flat wall, impacts and leaves the area of impact in two directions along the x-axis.

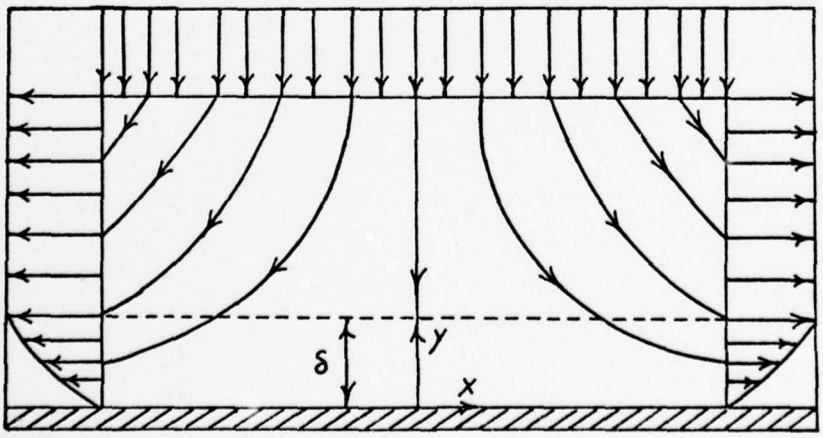

Figure 2. Stagnation in Plane Flow (From Ref 3: 88)

For the potential flow, the pressure was given by Bernoulli's equation

$$P_o - P = \tfrac{1}{2}\rho(U_e^2 + V_e^2) = \tfrac{1}{2}\rho a^2(x^2+y^2)$$

A similarity solution was assumed

$$u = x f'(y)$$
$$v = -f(y)$$
$$P_o - P = \tfrac{1}{2}\rho a^2 (x^2 + F(y))$$

which identically satisfied the continuity equation. The differential equations for f and F from the Navier-Stokes equations were

$$f'^2 - ff'' = a^2 + \nu f''' \qquad (30)$$
$$ff' = \tfrac{1}{2}a^2 F' - \nu f'' \qquad (31)$$

The boundary conditions at the wall, where u=v=0, and at a large distance from the wall, where $u=U_e=ax$, determined the boundary conditions on f and F.

$$f = f' = F = 0 \qquad \text{at } y = 0 \qquad (32)$$
$$f' = a \qquad \text{at } y = \infty \qquad (33)$$

A solution for f was determined first from Eq 30 by solving it numerically since it could not be solved in closed form. Equation 30 was non-dimensionalized by assuming

$$\eta = \alpha y$$
$$f(y) = A\phi(\eta)$$

where

$$\alpha = \sqrt{\frac{a}{\nu}}$$
$$A = \sqrt{\nu a}$$

This led to the differential equation

$$\phi''' + \phi\phi'' - \phi'^2 + 1 = 0$$

where ' denotes differentiation with respect to η . The boundary conditions were converted to

$$\phi = \phi' = 0 \qquad \text{at } \eta = 0$$
$$\phi' = 1 \qquad \text{at } \eta = \infty$$

Thus, the velocity component, u, became

$$\frac{u}{U_e} = \frac{1}{a} f'(y) = \phi'(\eta) \tag{34}$$

As η increased, $\phi'(\eta)$ increased linearly at first and then asymptotically approached one. At η = 2.4 the value of $\phi'(\eta)$ was approximately 0.99 or within one per cent of the final value. If the boundary layer edge is defined to be the value of $y = \delta$ where $u = 0.99\ U_e$, then

$$\delta = \eta_\delta \sqrt{\frac{\nu}{a}} \tag{35}$$

where η_δ was that value of η where $u = 0.99\ U_e$. A complete table of η, ϕ, ϕ' and ϕ'' is found in Schlichting (Ref 3: 90).

Approximate Solution from the Extended Momentum Integral Equation

The flow in the vicinity of the stagnation point was characterized by the external velocity distribution

$$U = 2\,x/l$$

or in dimensionless coordinates

$$U = 2\,\xi \tag{36}$$

With Eq 36 applied to the appropriate differential equations in Table I, the stagnation point equations were developed and recorded in Table VI. Removal of Reynolds number was not possible since Reynolds number is contained in the definition of J. To numerically integrate, it was necessary to determine initial values for δ_1, δ_1', ξ , and the quantities

Table VI

Stagnation Point Equations

Third Degree Velocity Profile

Extended Boundary Layer	$\delta_1'' = \delta_1'\left[\frac{(39-J/2-J^2/6)2\xi Re}{35(3-J/6)} - \frac{2}{\xi}\right] + \delta_1\left[\left\{\frac{2(39-J/2-J^2/6)}{35(3-J/6)}+1\right\}2Re + \frac{(5-J+J^2/36)2\xi J'Re}{35(9-J+J^2/36)}\right] - \frac{(9+J-J^2/12)}{16\delta_1}$ (37)
Boundary Layer	$\delta_1' = -\delta_1\left[\frac{J'(5-J+J^2/36)}{(39-J/2-J^2/6)(3-J/6)} + \frac{35(3-J/6)}{(39-J/2-J^2/6)}\left\{\frac{2(39-J/2-J^2/6)}{35(3-J/6)}+1\right\}\frac{1}{\xi}\right] + \frac{35(3-J/6)(9+J-J^2/12)}{32\delta_1 Re\,\xi(39-J/2-J^2/6)}$ (38)

Fourth Degree Velocity Profile

Extended Boundary Layer	$\delta_1'' = \delta_1'\left[\frac{20\xi Re(37/315-J/945-J^2/9072+1171K/3780+5JK/9072-19K^2/22680)}{(3-J/12+K/4)} - \frac{2}{\xi}\right] + \delta_1\left[2Re\left\{\frac{20(37/315-J/945-J^2/9072+1171K/3780}{(3-J/12+K/4)}\right.\right.$ $\left.+5JK/9072-19K^2/22680)}{(3-J/12+K/4)}+1\right\} + 20\xi Re\left\{\frac{(3-J/12+K/4)(-J'/945-JJ'/4536+1171K'/3780+5JK'/9072+5J'K/9072-19KK'/11340)}{(3-J/12+K/4)^2}\right.$ $\left.\left.-\frac{(37/315-J/945-J^2/9072+1171K/3780+5JK/9072-19K^2/22680)(-J'/12+K'/4)}{(3-J/12+K/4)^2}\right\}\right] - \frac{(2+J/6-K/6)(3-J/12+K/4)}{10\delta_1}$ (39)
Boundary Layer	$\delta_1' = -\delta_1\left[\frac{(3-J/12+K/4)(-J'/945-JJ'/4536+1171K'/3780+5JK'/9072+5J'K/9072-19KK'/11340)}{(3-J/12+K/4)(37/315-J/945-J^2/9072+1171K/3780+5JK/9072-19K^2/22680)} - \frac{(37/315-J/945-J^2/9072+1171K/3780}{(3-J/12+K/4)(37/315-J/945-J^2/9072+1171K/3780+5JK/9072-19K^2/22680)}\right.$ $\left.+5JK/9072-19K^2/22680)(-J'/12+K'/4)}{10\xi(37/315-J/945-J^2/9072+1171K/3780+5JK/9072-19K^2/22680)} + \frac{(3-J/12+K/4)}{10\xi(37/315-J/945-J^2/9072+1171K/3780+5JK/9072-19K^2/22680)}$ $\left\{\frac{20(37/315-J/945-J^2/9072+1171K/3780+5JK/9072-19K^2/22680)}{(3-J/12+K/4)}+1\right\}\Big] +$ $\frac{(2+J/6-K/6)(3-J/12+K/4)^2}{200\,Re\,\delta_1\xi(37/315-J/945-J^2/9072+1171K/3780+5JK/9072-19K^2/22680)}$ (40)

J and K. For the exact solution, Eq 35, δ did not vary with x or ξ; therefore, δ_1 was also constant and one of the initial conditions prescribed was that

$$\delta_1' = 0 \qquad \text{at } \xi = 0.0001$$

where the value of ξ was chosen arbitrarily small. The value of K was zero since $U_{\xi\xi}$ from Eq 36 is zero. From Eq 17, the J equation for stagnation point flow became

$$J = 2(\delta/\ell)^2 Re \tag{41}$$

Using the expressions in Table I for the displacement thickness, δ_1, a relationship between J and δ_1 was derived for each profile. These relationships were

$$J = \frac{128\,\delta_1^2 Re}{9 - J + J^2/36} \tag{42}$$

for the third degree velocity profile and

$$J = \frac{200\,\delta_1^2 Re}{9 - J/2 + J^2/144} \tag{43}$$

for the fourth degree velocity profile. Thus, for a given Reynolds number, the values of J and δ_1 must satisfy Eq 42 or Eq 43. The possibility existed that J would have three values (roots) for a given δ_1 and Reynolds number.

Determination of Initial Values for J and δ_1

With δ_1 constant for the stagnation point flow, the following condition was implied:

$$\delta_1'' = \delta_1' = 0 \qquad \text{at } \xi \approx 0 \tag{44}$$

From Eq 41 or the complementary equations, Eq 42 or Eq 43, the value of J was also constant for a given Reynolds number. Thus,

$$J' = 0 \tag{45}$$

Using the conditions of Eq 44 and Eq 45, the extended boundary layer equations in Table VI were reduced to functions of δ_1, J and Reynolds number. These new equations were then used with Eq 42 or Eq 43 to solve for J and then δ_1. For the fourth degree velocity profile Eq 44 and Eq 45 were imposed on Eq 39 with the following result:

$$0 = \delta_1\left[2\,Re\left\{\frac{20(37/315 - J/945 - J^2/4072)}{(3 - J/12)} + 1\right\}\right] - \frac{(2+J/6)(3-J/12)}{10\,\delta_1}$$

or, after rearranging,

$$20\,\delta_1^2 Re = \frac{(2+J/6)(3-J/12)^2}{33/63 - 79J/756 - 5J^2/2268} \tag{46}$$

Substituting Eq 46 into Eq 43 gave

$$J = \frac{10(2+J/6)}{33/63 - 79J/756 - 5J^2/2268} \tag{47}$$

which is a third degree equation for J. The roots of J for both the fourth degree and third degree velocity profiles are given in Table VII.

Table VII

Values of J and $\delta_1^2 Re$ Satisfying Equation 44 and Equation 42 or Equation 43

Third Degree Velocity Profile (42)		Fourth Degree Velocity Profile (43)	
J	$\delta_1^2 Re$	J	$\delta_1^2 Re$
5.8653997 + 2.1656705 i	85.814115 + 0.0126237 i	7.0523231	0.20519518
5.8653997 - 2.1656705 i	85.814115 - 0.0126237 i	17.803257	0.2046889
-32.230799	-17.648133	-72.255580	-29.402177

From Eq 41, J must be real and positive; therefore, a solution for the third degree velocity profile that meets the required conditions for the stagnation point was not possible. The reason for this is not understood at this time. For the fourth degree velocity profile two

roots for J seemed plausible:

$$J_1 = 7.0523231$$
$$J_2 = 17.803257$$

From the exact solution discussed previously and in Schlichting (Ref 3: 89) a relationship was developed between J and η_δ. Equation 41 was rewritten as follows:

$$J = 2(\delta/\ell)^2 Re = 2(\delta/\ell)^2 \frac{U_\infty \ell}{\nu} = \delta^2 \left(\frac{a}{\nu}\right)$$

where "a" was transformed from

$$a = U_e/x$$

to

$$a = 2U_\infty/\ell$$

Applying Eq 35 gave

$$J = \eta_\delta^2 \tag{48}$$

Corresponding values of η_δ were computed for J_1 and J_2 from Eq 48. The η values in Table 5.1 of Schlichting (Ref 3: 90) were redefined to correspond to $\eta = y/\delta$ used in the assumed velocity profiles by dividing the η in the table by the computed η_δ for the respective J value. With the exact solution now defined in the same terms as the approximate solution, a comparison was made between the two solutions based on the J value. These comparisons are presented in Figures 3 and 4.

Both J_1 and J_2 were tried as the J value for the stagnation point. For a given Reynolds number, δ_1 was derived from Eq 43 (See Table VII). Thus, the required initial conditions were

$$\delta_1' = 0 \qquad \delta_1' = 0$$
$$J_1 = 7.0523231 \qquad J_2 = 17.803257$$
$$\delta_1 = \sqrt{0.20519518/Re} \qquad \delta_1 = \sqrt{0.2046889/Re}$$

and the integration of Eq 39 was begun.

Results

Throughout the range of integration, δ_1 remained constant or nearly so for both the extended boundary layer and boundary layer solutions. This demonstrated that the equations satisfied the conditions at or near the stagnation point. With the starting conditions defined, the stagnation point results were used as initial conditions for the circular cylinder flow.

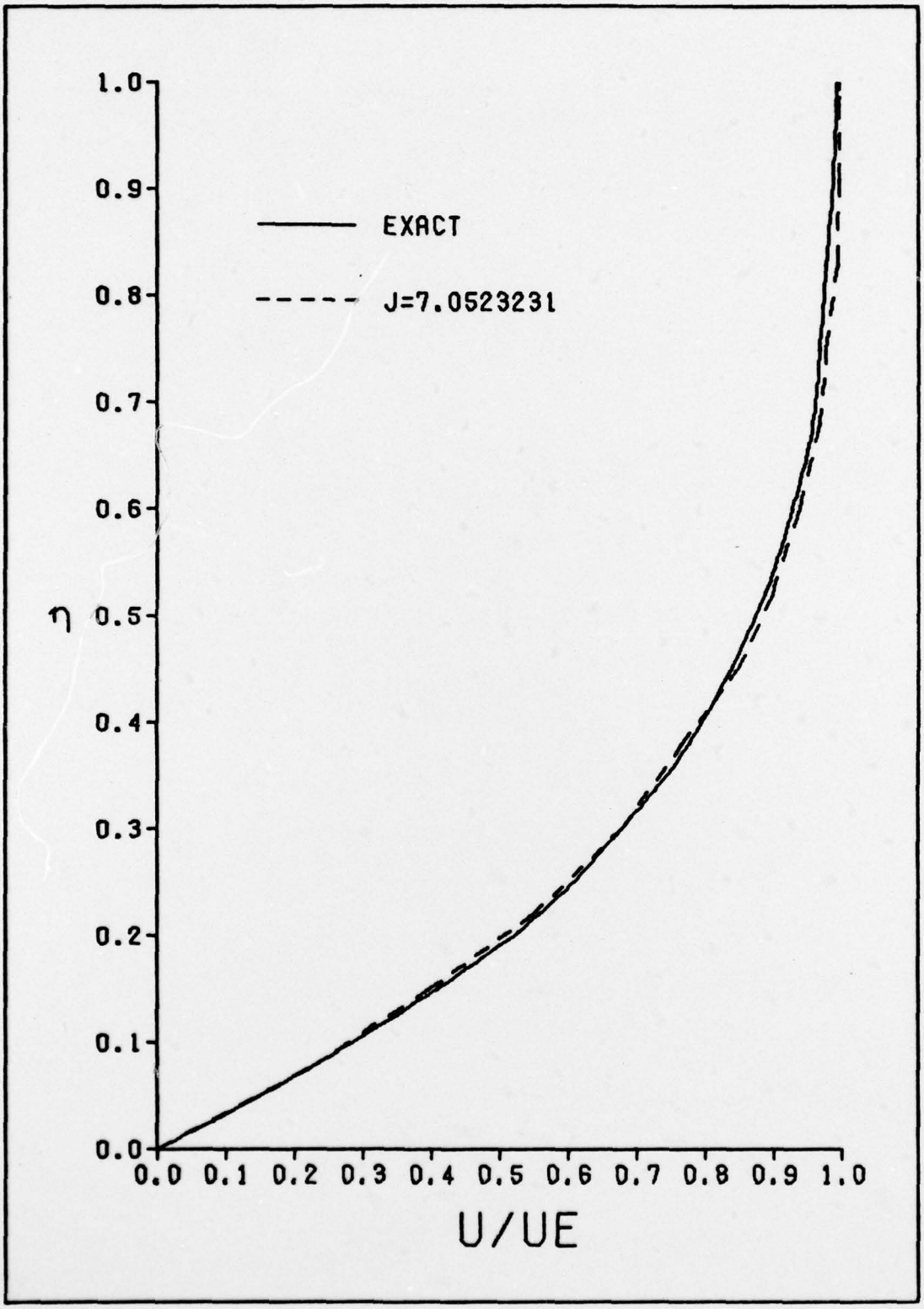

Figure 3. Comparison of Velocity Distributions for Exact Solution and Fourth Degree Profile Solution with J = 7.0523231

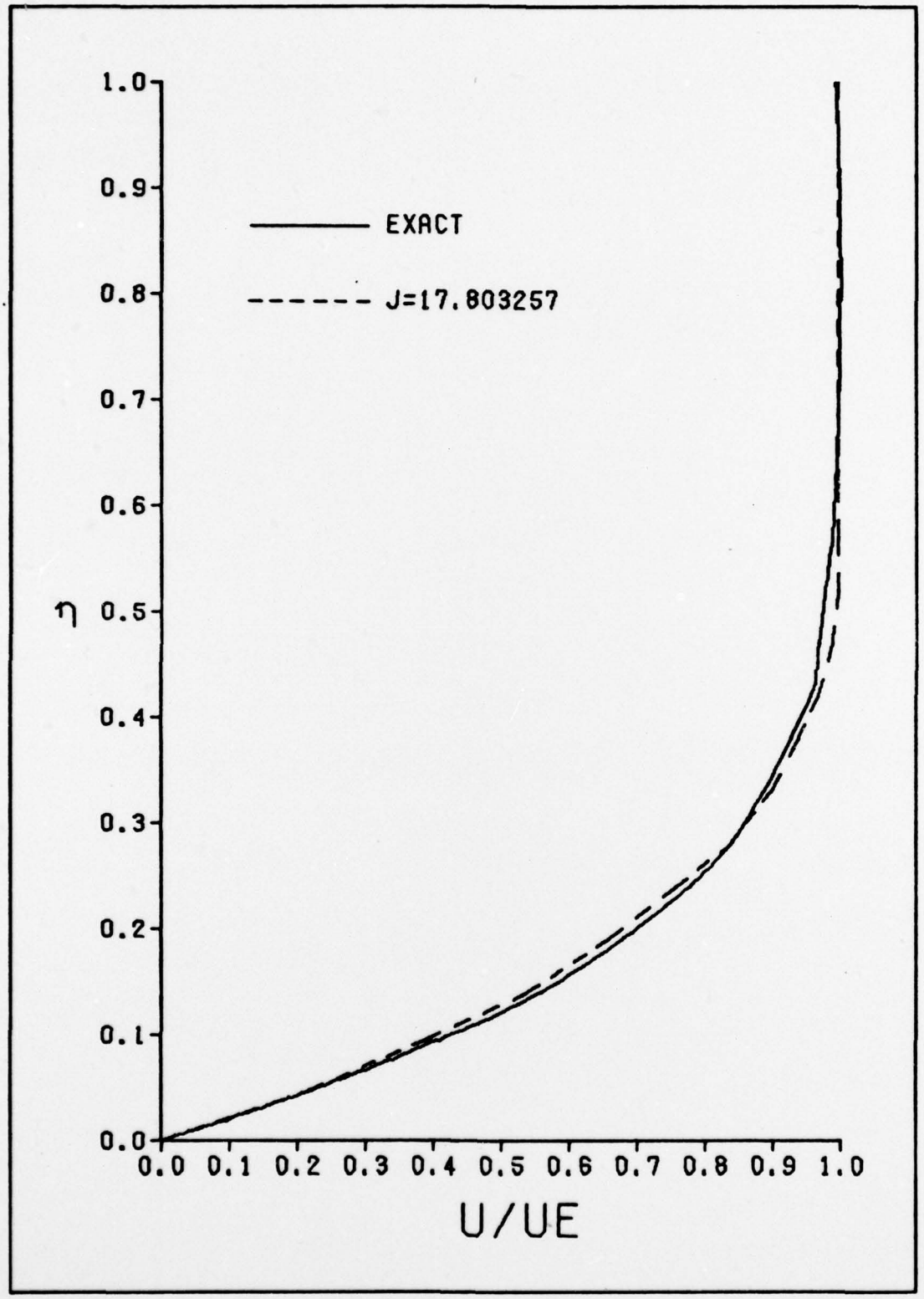

Figure 4. Comparison of Velocity Distributions for Exact Solution and Fourth Degree Profile Solution with J = 17.803257

V. Circular Cylinder Solution

Introduction

The flow around a circular cylinder is a classical case for testing viscous equation solution methods as it permits the study of a boundary layer from a stagnation point through a separation point. The flow is characterized by the external velocity distribution

$$U = 2 \sin (X/R)$$

or in dimensionless coordinates,

$$U = 2 \sin \xi$$

where ξ is the angle in radians measured from the stagnation point and R is the cylinder radius now used as the characteristic length. The discussion is limited to the solution for the assumed fourth degree velocity profile since the conditions at the stagnation point for the third degree velocity profile were undetermined. The equations for the circular cylinder are listed in Table VIII.

With the given pressure distribution the values of J and K were as follows:

$$J = \frac{200 \delta_1^2 Re \cos \xi}{(3 - J/12 + K/4)^2} \tag{49}$$

$$K = \frac{-100 \delta_1^2}{(3 - J/12 + K/4)^2} = \frac{-J}{2 Re \cos \xi} \tag{50}$$

The initial conditions imposed for this case were taken from the stagnation point results

$$\delta_1' = 0 \qquad \text{at } \xi = 0.0001$$

$$J = 7.0523231 \quad \text{or} \quad J = 17.803257$$

where the initial value of ξ was arbitrarily selected. The initial

Table VIII

Circular Cylinder Equations for Fourth Degree Velocity Profile

Extended Boundary Layer	$\delta_1'' = \delta_1' \left[\frac{20\,Re \sin\xi \left(\frac{37}{315} - \frac{J}{945} - \frac{J^2}{9072} + \frac{1171K}{3780} + \frac{5JK}{9072} - \frac{19K^2}{22680}\right)}{\left(3 - \frac{J}{12} + \frac{K}{4}\right)} - \frac{2\cos\xi}{\sin\xi} \right] + \delta_1 \left[2\,Re \cos\xi \left\{ \frac{\left(\frac{37}{315} - \frac{J}{945} - \frac{J^2}{9072} + \frac{1171K}{3780} + \frac{5JK}{9072} - \frac{19K^2}{22680}\right)}{\left(3 - \frac{J}{12} + \frac{K}{4}\right)} + 1 \right\} - \left\{ \frac{10}{\left(3 - \frac{J}{12} + \frac{K}{4}\right)} - 1 \right\} + 20\,Re \sin\xi \left\{ \frac{\left(3 - \frac{J}{12} + \frac{K}{4}\right)\left(-\frac{J'}{945} - \frac{JJ'}{4536} + \frac{1171K'}{3780} + \frac{5JK'}{9072} + \frac{5J'K}{9072} - \frac{19KK'}{11340}\right) - \left(\frac{37}{315} - \frac{J}{945} - \frac{J^2}{9072}\right)}{\left(3 - \frac{J}{12} + \frac{K}{4}\right)^2} + \frac{1171K}{3780} + \frac{5JK}{9072} - \frac{19K^2}{22680}\left(-\frac{J'}{12} + \frac{K'}{4}\right) \right\} \right] - \frac{\left(2 + \frac{J}{6} - \frac{K}{6}\right)\left(3 - \frac{J}{12} + \frac{K}{4}\right)}{10\,\delta_1}$ (51)
Boundary Layer	$\delta_1' = \delta_1 \left[\frac{25J'\left(\frac{3}{10} - \frac{J}{120}\right)\left(1 - \frac{J}{10} + \frac{J^2}{120}\right)}{378\left(\frac{37}{315} - \frac{J}{945} - \frac{J^2}{9072}\right)\left(9 - \frac{J}{2} + \frac{J^2}{144}\right)} - \frac{\left(\frac{3}{10} - \frac{J}{120}\right)}{\left(\frac{37}{315} - \frac{J}{945} - \frac{J^2}{9072}\right)} \left\{ \frac{2\left(\frac{37}{315} - \frac{J}{945} - \frac{J^2}{9072}\right)}{\left(\frac{3}{10} - \frac{J}{120}\right)} + 1 \right\} \frac{\cos\xi}{\sin\xi} \right] + \frac{\left(\frac{3}{10} - \frac{J}{120}\right)\left(3 + \frac{J}{6} - \frac{J^2}{144}\right)}{10\,\delta_1\,Re\left(\frac{37}{315} - \frac{J}{945} - \frac{J^2}{9072}\right)\sin\xi}$ (52)

values of K and δ_1 were then computed based on the selected J value and Reynolds number.

Results

With the initial values computed, the integration was begun and proceeded until δ_1 became greater than 10^4 or until ξ equaled 3.14, indicating the aft portion of the cylinder had been reached. The extended boundary layer and boundary layer solutions were integrated at Reynolds numbers of 1, 10, 100, and 1000. For a given Reynolds number, the extended boundary layer and boundary layer solutions began from nearly the same value of δ_1. However, δ_1'' was not zero or nearly zero for the extended boundary layer solution near the stagnation point as was the case for the stagnation point flow. This was the result of the term, U"/U, in Eq 22 no longer being zero. This term caused δ_1'' to have a large negative value and the extended boundary layer solution (δ_1) decayed rather quickly for the fourth degree velocity profile as depicted in Figure 5. Meanwhile, the boundary layer solution had δ_1 increasing gradually until a certain angle from the stagnation point, ϕ, was approached, at which time the δ_1 increased rapidly and exceeded 10^4. The higher the Reynolds number, the higher was the value of ϕ where δ_1 increased rapidly. The point of rapid δ_1 increase was assumed to be where separation occurs. As shown in Figure 5, the angle ϕ was in the range of 130 degrees to 150 degrees for the Reynolds numbers tested rather than approximately 82 degrees as previous studies have shown (Ref 3: 202). Thus, the present results are not understood.

A possible reason for this conflict could be the coordinate system used. A rectangular coordinate system does not account for the curvature of the cylinder. This could impact the solution for the extended

boundary layer and boundary layer approaches dramatically. Perhaps it would have been more appropriate to have used a cylindrical coordinate system thereby accounting for the curvature.

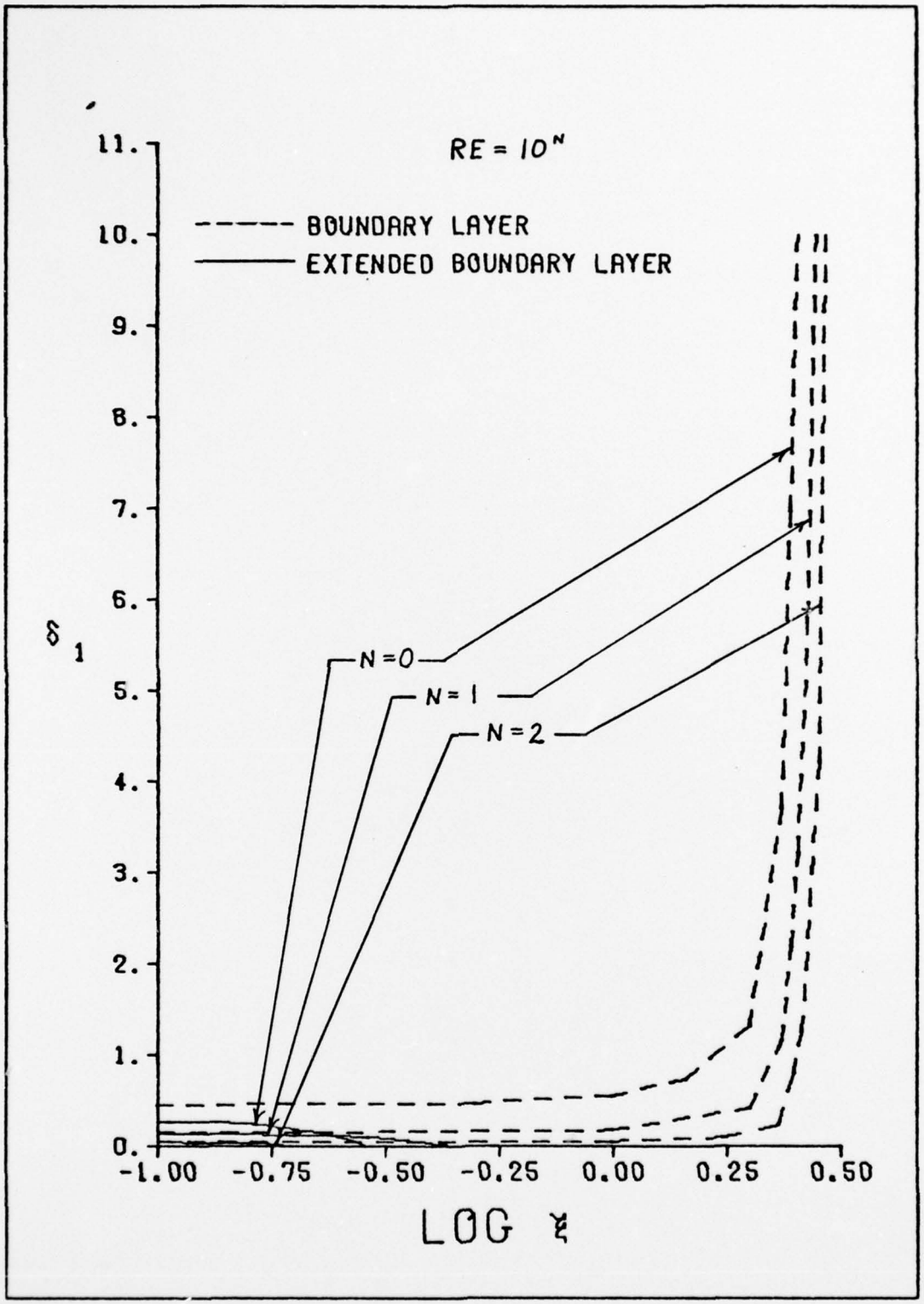

Figure 5. Comparison of Extended Boundary Layer and Boundary Layer Solutions for Reynolds Numbers of 1, 10, and 100

VI. Conclusions and Recommendations

Conclusions

The conclusions drawn from this study of the extended boundary layer equations are presented as follows:

1. A momentum integral equation can be developed which includes the streamwise diffusion term. It is hypothesized that this is a more accurate approach than the boundary layer equations and a necessary approach for boundary layer flows near separation.

2. The results obtained for the flow over a flat plate were in agreement with those presented in other studies.

3. The results obtained for the flow at the stagnation point and over a circular cylinder were less than satisfactory. The extended boundary layer and boundary layer solutions did not agree for the flow over a cylinder at any Reynolds number.

4. The method applied did not give a clear indication as to where separation occurred on the cylinder as compared to previously demonstrated methods.

Recommendations

The following recommendations are made for future studies in this area:

1. The coordinate system used in the extended boundary layer equations should be changed to a cylindrical coordinate system, appropriate equations developed, and the same tests run to determine whether correct results could be obtained.

2. The y-momentum equation should be solved for the normal pressure gradient term to determine whether it is negligibly small as assumed.

Bibliography

1. Ketter, Robert L. and Sherwood P. Prawel, Jr. Modern Methods of Engineering Computation. New York: McGraw-Hill Book Company, 1969.

2. Koob, Stephen J. and Douglas E. Abbott. An Integral-Differential-Difference Method Analysis of Viscous Flow Over an Impulsively Accelerated Semi-Infinite Plate. Purdue University Mechanical Engineering Report, Technical Report FMTR-68-2, December, 1968.

3. Schlichting, Hermann. Boundary Layer Theory (Sixth Edition). New York: McGraw-Hill Book Company, 1968.

Vita

Robert D. Behr was born on 30 March 1946 in Cincinnati, Ohio. He graduated from Colerain High School, Cincinnati, Ohio in 1964. He attended the United States Air Force Academy from which he received a Bachelor of Science degree in Aeronautical Engineering and a commission in the United States Air Force in 1968. He received an aeronautical rating of navigator at Mather Air Force Base, California in 1969. He has served as a navigator with the 62nd Military Airlift Wing, McChord AFB, Washington, and the 362nd Tactical Electronic Warfare Squadron, Danang AF, Republic of Vietnam. He then served as an instructor navigator and T45 Simulator test director in the 323rd Flying Training Wing, Mather AFB, California until entering the School of Engineering, Air Force Institute of Technology, in June 1976.

Permanent address: 3212 Floridale Lane
Cincinnati, Ohio 45239

UNCLASSIFIED

SECURITY CLASSIFICATION OF THIS PAGE (When Data Entered)

REPORT DOCUMENTATION PAGE	READ INSTRUCTIONS BEFORE COMPLETING FORM
1. REPORT NUMBER: AFIT/GAE/AA/77D-1	2. GOVT ACCESSION NO. / 3. RECIPIENT'S CATALOG NUMBER
4. TITLE (and Subtitle): APPLICATION OF THE KARMAN-POHLHAUSEN METHOD TO THE EXTENDED BOUNDARY LAYER EQUATIONS.	5. TYPE OF REPORT & PERIOD COVERED: MS THESIS; Master's thesis
	6. PERFORMING ORG. REPORT NUMBER
7. AUTHOR(s): Robert D. Behr, Captain USAF	8. CONTRACT OR GRANT NUMBER(s)
9. PERFORMING ORGANIZATION NAME AND ADDRESS: Air Force Institute of Technology (AFIT/EN), Wright-Patterson, AFB, OH 45433	10. PROGRAM ELEMENT, PROJECT, TASK AREA & WORK UNIT NUMBERS
11. CONTROLLING OFFICE NAME AND ADDRESS: Air Force Institute of Technology (AFIT/EN), Wright-Patterson AFB, OH 45433	12. REPORT DATE: Dec 1977; 13. NUMBER OF PAGES: 43 (12) 46p.
14. MONITORING AGENCY NAME & ADDRESS (if different from Controlling Office)	15. SECURITY CLASS. (of this report): UNCLASSIFIED; 15a. DECLASSIFICATION/DOWNGRADING SCHEDULE

16. DISTRIBUTION STATEMENT (of this Report)

Approved for public release; distribution unlimited.

17. DISTRIBUTION STATEMENT (of the abstract entered in Block 20, if different from Report)

18. SUPPLEMENTARY NOTES: Approved for public release; IAW AFR 190-17

JERRAL F. GUESS, Captain, USAF
Director of Information

19. KEY WORDS (Continue on reverse side if necessary and identify by block number)

Boundary Layer equations
Navier-Stokes equations
Two-dimensional boundary layer
Boundary layer flow

AD A12 225

20. ABSTRACT (Continue on reverse side if necessary and identify by block number)

An analytical study of the application of the Karman-Pohlhausen method to the extended boundary layer equations at low Reynolds number was made. The extended boundary layer equations were the incompressible Navier-Stokes equations with the assumption of zero normal pressure gradient. A comparison was made between the solutions for the extended boundary layer equations and the boundary layer equations at several Reynolds numbers for flow over a flat plate, flow near a stagnation point, and flow over a circular cylinder.

DD FORM 1 JAN 73 1473 EDITION OF 1 NOV 65 IS OBSOLETE

UNCLASSIFIED

SECURITY CLASSIFICATION OF THIS PAGE (When Data Entered)

Favorable results were achieved for the flat plate case while less than satisfactory results were achieved for the circular cylinder. The point of separation was not found. Any further study in this area should consider using cylindrical coordinates for the cylinder solution and examining the effect of the pressure gradient normal to the body.